Eigenvalue problem for the Quantum Harmonic Oscillator

Rama Khalil

April 6, 2025

Contents

1 Introduction

This project delves into solving the time-independent Schrödinger equation for the one-dimensional quantum harmonic oscillator using two different numerical methods: the finite-difference diagonalization, FD, and the inverse power iteration, IPI.
To estimate the accuracy and efficiency of both approaches, the computed eigenvalues and eigenvectors are compared against analytical solutions. Additional analysis includes runtime comparsion and orthonormality checks. Lastly, we introduce a time-dependency by growing a bump in the middle of the harmonic potential and analyze how the corresponding eigenvalues and eigenstates are effected.

2 Theory

2.1 Time-dependent Schrödinger equation

Given some initial conditions, usually at $t = 0$, the particle's wave function at future time, $\psi(x, t)$, is obtained by solving Schrödinger equation:

$$i\hbar\frac{\partial}{\partial t}\psi = \hat{H}\psi \tag{1}$$

Where $\hat{H}$ is the Hamiltonian operator [1], which in one-dimensions is:

$$\hat{H} = -\frac{\hbar^2}{2m}\frac{\partial^2}{\partial x^2} + V(x,t) \tag{2}$$

2.2 Algebraic solution to the Quantum Harmonic Oscillator

We will start with a time-independent system, that of the harmonic oscillator.
The harmonic oscillator model gives a good first approximation in the neighborhood of a local minimum, say $x = x_0$. The potential in one dimension can therefore be expanded in a Taylor series about the minimum:

$$V(x) = V(x_0) + V'(x_0)(x - x_0) + \frac{1}{2}V''(x_0)(x - x_0)^2 + ... \tag{3}$$

Since $x = x_0$ is a minimum, we can set $V'(x_0) = 0$ and $k = V''(x_0)$:

$$V(x) - V(x_0) \quad \approx \quad \frac{1}{2}k(x - x_0)^2 \tag{4}$$

By rearranging (5) and setting it in (2), the Hamiltonian operator can be written as follows:

$$\hat{H} = -\frac{\hbar^2}{2m}\frac{\partial^2}{\partial x^2} + \frac{1}{2}m\omega^2 x^2 \tag{5}$$

Using the momentum operator $\hat{p} \equiv i\hbar d/dx$ and factoring the Hamiltonian gives the following form of the time-independent Schrödinger equation:

$$\frac{1}{2m}\left[\hat{p}^2 + (mw\hat{x})^2\right]\psi = E\psi \tag{6}$$

To find the solutions, the following operators are introduced [2]:

$$\hat{a}_\pm \equiv \frac{1}{\sqrt{2\hbar m\omega}}(\mp i\hat{p} + mw\hat{x}) \tag{7}$$

Multiplying the lowering operator with the rising operator (in this specific order since operators are not

[1] The total energy, sum of kinetic and potential energy operators.
[2] Ladder operators: used to climb up and down in energy.

commutative):

$$\hat{a}_-\hat{a}_+ = \frac{1}{2\hbar m\omega}\left[\hat{p}^2 + (m\omega\hat{x})^2 - im\omega(\hat{x}\hat{p} - \hat{p}\hat{x})\right] \tag{8}$$

Note that the last term in the bracket is the commutator of $\hat{x}$ and $\hat{p}$:

$$\hat{a}_-\hat{a}_+ = \frac{1}{2\hbar m\omega}\left[\hat{p}^2 + (m\omega\hat{x})^2\right] - \frac{i}{2\hbar}\left[\hat{x}, \hat{p}\right] \tag{9}$$

The last term is nothing but the canonical commutation relation [3]:

$$\left[\hat{x}, \hat{p}\right] = i\hbar \tag{10}$$

Putting all of this together, the Hamiltonian can be written as follows:

$$\hat{H} = \hbar\omega\left(\hat{a}_+\hat{a}_- + \frac{1}{2}\right) \tag{11}$$

And the Schrödinger equation in terms of $\hat{a}_\pm$ takes the form

$$\hbar\omega\left(\hat{a}_\pm\hat{a}_\mp \pm \frac{1}{2}\right)\psi = E\psi \tag{12}$$

To find the ground state wave function and energy, we will use the fact that when the lowering operator operates on the ground state, we get zero:

$$\hat{a}_-\psi_0 = 0 \tag{13}$$

Using this in equation (7) gives a differential equation with the following solution (after normalization):

$$\psi_0(x) = \left(\frac{m\omega}{\pi\hbar}\right)^{1/4} e^{-\frac{m\omega}{2\hbar}x^2} \tag{14}$$

The ground state energy is obtained by setting this in equation (13) and solving for E:

$$E_0 = \frac{1}{2}\hbar\omega \tag{15}$$

The excited states can be found by applying the rising operator repeatedly

$$\boxed{\psi_n(x) = A_n(\hat{a}_+)^n\psi_0(x)} \tag{16}$$

Where A_n is the normalization constant. The energy of an arbitrary state:

$$\boxed{E_n = \left(n + \frac{1}{2}\right)\hbar\omega} \tag{17}$$

In this assignment, reduced units will be used to make equations and calculations easier and more straightforward. This means that lengths will be measured in units of $\sqrt{\frac{\hbar\omega}{m}}$ and energies in units of $\hbar\omega$. Time will then be given in units of $1/\omega$. Consequently, the harmonic oscillator will be oscillating with the angular frequency 1.

[3] David J. Griffiths. Introduction to quantum mechanics, (3rd edition): Cambridge University Press.

2.3 Perturbing the system

The quantum system is now perturbed by adding an additional potential term to the Hamiltonian, the system is then time propagated, the new Hamiltonian can now be written as:

$$\hat{H}(t) = \hat{H}_\omega(x) + V(x,t) \tag{18}$$

2.3.1 Symmetric Gaussian potential

To maintain simplicity, consider the perturbation as a Gaussian-shaped bump introduced into the harmonic oscillator potential, and positioned at its midpoint.
The general form of a Gaussian function is:

$$V(x) = C_1 e^{-C_2 x^2} \tag{19}$$

Where the values of C_1 and C_2 will be chosen in a way such that a particle at the lowest energy levels will have to tunnel through the bump in order to go from one side to the other. The total potential is shown in the figure below

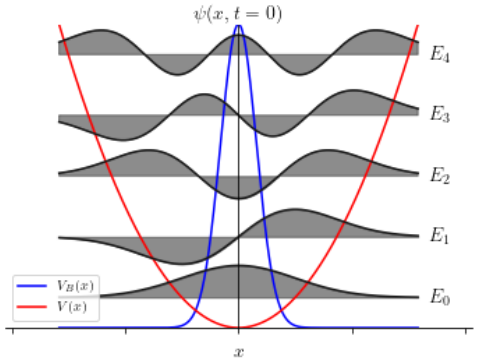

(a) The Harmonic potential along with the symmetric Gaussian potential.

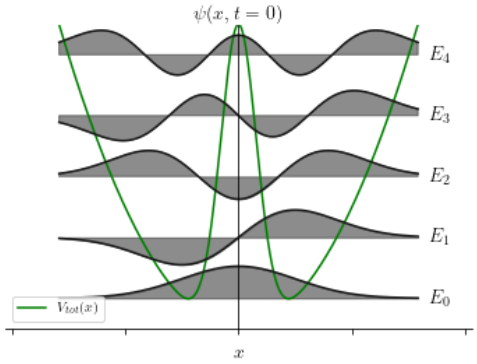

(b) The effective potential acting on the system.

In future sections, the constants will take the following values:

$$C_1 = 10 \quad \text{and} \quad C_2 = 5 \tag{20}$$

3 Numerical methods

3.1 Finite difference method, FDM

The finite difference method is a numerical tool used to approximate solutions to differential equations by approximating derivatives with finite differences. In the case of Schrödinger equation, the continuous spatial domain is discretized and therefore the differential equation is transformed into a set of linear equations, which can easily be solved numerically. This section describes the mathematical formulation of the finite difference method applied to the one-dimensional time-independent Schrödinger equation. Recall equation (2), which with a time-independent potential is:

$$\hat{H} = -\frac{\hbar^2}{2m}\frac{\partial^2}{\partial x^2} + \frac{1}{2}m\omega^2\hat{x}^2 \tag{21}$$

Introducing the dimensionless quantity $z = x\sqrt{\frac{m\omega}{\hbar}}$ to factorize the Hamiltonian as:

$$\hat{H} = \frac{\hbar\omega}{2}\Big(\frac{\partial^2}{\partial z^2} + z^2\Big) \tag{22}$$

Schrödinger equation can be written as follows:

$$\frac{1}{2}\Big(\frac{\partial^2}{\partial z^2} + z^2\Big)\Psi = \frac{E}{\hbar\omega}\Psi \tag{23}$$

Now, the finite difference approximation is used to express the second derivative in terms of the function itself. It assumes that the function can be expanded in a Taylor series around the desired point. Considering the wave function is defined at x, its values in the vicinity can be expanded as:

$$\begin{aligned}\Psi(x \pm h) &= \Psi(x) \pm h\Psi'(x) + \frac{h^2}{2}\Psi''(x) \pm \frac{h^3}{6}\Psi^{(3)}(x) + \frac{h^4}{24}\Psi^{(4)}(x) + \mathcal{O}(h^5)\\ \Psi(x \pm 2h) &= \Psi(x) \pm 2h\Psi'(x) + 2h^2\Psi''(x) \pm \frac{4h^3}{3}\Psi^{(3)}(x) + \frac{2h^4}{3}\Psi^{(4)}(x) + \mathcal{O}(h^5)\end{aligned} \tag{24}$$

Combining these expansions appropriately, we obtain a more accurate expression for the second derivative — the **five-point stencil**:

$$\frac{\partial^2\Psi(x)}{\partial x^2} = \frac{-\Psi(x-2h) + 16\Psi(x-h) - 30\Psi(x) + 16\Psi(x+h) - \Psi(x+2h)}{12h^2} + \mathcal{O}(h^4) \tag{25}$$

This improves the accuracy of the second derivative approximation from $\mathcal{O}(h^2)$ (in the three-point stencil) to $\mathcal{O}(h^4)$. Now, the time-independent 1D Schrödinger equation becomes:

$$-\frac{1}{2}\frac{\partial^2\Psi(x)}{\partial x^2} + V(x)\Psi(x) = E\Psi(x) \tag{26}$$

Plugging in equation (22) into (23):

$$-\frac{1}{2}\cdot\frac{1}{12h^2}\left[-\Psi(x-2h) + 16\Psi(x-h) - 30\Psi(x) + 16\Psi(x+h) - \Psi(x+2h)\right] + V(x)\Psi(x) = E\Psi(x) \tag{27}$$

Scaling the potential and energy values by a factor of 2

$$\frac{1}{12h^2}\left[-\Psi(x-2h) + 16\Psi(x-h) - 30\Psi(x) + 16\Psi(x+h) - \Psi(x+2h)\right] + 2V(x)\Psi(x) = 2E\Psi(x) \tag{28}$$

Note that by scaling the energy by a factor 2, the energy values will instead be given by:

$$\boxed{E_n = 2n + 1} \tag{29}$$

Multiplying through and discretizing leads to a Hamiltonian operator of the form:

$$\hat{H} = \frac{1}{12h^2} \begin{pmatrix} -30 & 16 & -1 & 0 & \cdots & 0 \\ 16 & -30 & 16 & -1 & \ddots & \vdots \\ -1 & 16 & -30 & 16 & \ddots & 0 \\ 0 & \ddots & \ddots & \ddots & \ddots & -1 \\ \vdots & \ddots & -1 & 16 & -30 & 16 \\ 0 & \cdots & 0 & -1 & 16 & -30 \end{pmatrix} \tag{30}$$

Note that the matrix is now **pentadiagonal**, symmetric, and banded, which allows for efficient sparse storage and linear algebra methods. The potential energy matrix is still diagonal, with the potential values at each grid point placed along the diagonal:

$$V(x) = \begin{pmatrix} V(x_1) & 0 & \cdots & 0 \\ 0 & V(x_2) & \cdots & 0 \\ \vdots & \vdots & \ddots & \vdots \\ 0 & 0 & \cdots & V(x_n) \end{pmatrix} \tag{31}$$

Finally, the total Hamiltonian is formed by adding the potential to the kinetic matrix. Diagonalizing the Hamiltonian yields the eigenvalues (energies) and eigenvectors (wave functions) of the system:

$$H\Psi = E\Psi \tag{32}$$

3.2 Inverse Power Iteration with a shift

To compute specific eigenvalues of the Hamiltonian without having to perform a full matrix diagonalization, we use the *IPI* method with a shift. This iterative technique is particularly effective for finding the eigenvalue closest to a given value ξ.
The idea is based on rewriting the eigenvalue problem:

$$A\vec{x}_n = \lambda_n \vec{x}_n \quad \Longleftrightarrow \quad A^{-1}\vec{x}_n = \lambda_n^{-1}\vec{x}_n \tag{33}$$

But since computing A^{-1} explicitly is still computationally expensive, we instead solve the equivalent linear system:

$$A\vec{y}_{i+1} = \vec{y}_i \tag{34}$$

This avoids the need for matrix inversion by using LU decomposition of A once, and to find eigenvalues near a desired value ξ, we just apply the method to the *shifted* matrix:

$$A \to A - \xi I \tag{35}$$

which transforms the eigenvalues as $\lambda_n \to \lambda_n - \xi$, allowing the algorithm to converge to the eigenvalue with minimum $|\lambda_n - \xi|$.

3.3 Limitations of the model

While our numerical approach yields highly accurate results, the model carries certain simplifications and approximations. These limitations fall into two main categories:

3.3.1 Physical limitations

Idealized harmonic potential In this model we use, $V(x) = x^2$, which is an idealization that assumes a perfectly quadratic and symmetric potential extending to infinity, which is not the case in real quantum systems.

3.3.2 Numerical limitations

Finite difference approximation The second derivative is approximated using a five-point finite difference stencil. Although this provides a relatively high-order accuracy ($\mathcal{O}(h^4)$), it still introduces uncertainty, which increases for higher excited states where the wavefunctions oscillate more rapidly.

Imposing Dirichlet boundary conditions The solutions are computed only on a finite domain, $x \in [x_{\min}, x_{\max}]$, and are assumed to vanish at the boundaries:

$$\Psi(x_{\min}) = \Psi(x_{\max}) = 0$$

While for the quantum harmonic oscillator, the true wavefunctions decay asymptotically but never reach exactly zero.

4 Results

4.1 Eigenvalues

The eigenvalues for the harmonic oscillator were computed using three different methods, the algebraic approach 2.2, the finite-difference method, and the inverse power iteration.
Table 1 presents a comparison of those methods, and to illustrate both the accuracy near the ground state and at higher excitations, we include the first and last three eigenvalues from a total of 30 computed states using $N_x = 2000$ grid points.

Table 1: Comparison of the first and last 3 eigenvalues.

n	Analytical	FD	IPI
0	1	0.99999999	0.99999999
1	3	2.99999994	2.99999994
2	5	4.99999984	4.99999984
27	55	54.99993651	54.99993651
28	57	56.99991177	56.99991177
29	59	58.99987904	58.99987904

As shown, both numerical methods achieve excellent agreement (up to 8 digits) with the analytical solution across the spectrum.

4.2 Eigenvectors

Similarly, Figure 2 and 3 shows the wave functions for the first and last three eigenvectors computed using FD and IPI. The finite-difference solutions are shown as dashed blue lines, while the inverse power iteration results are shown as solid red lines:

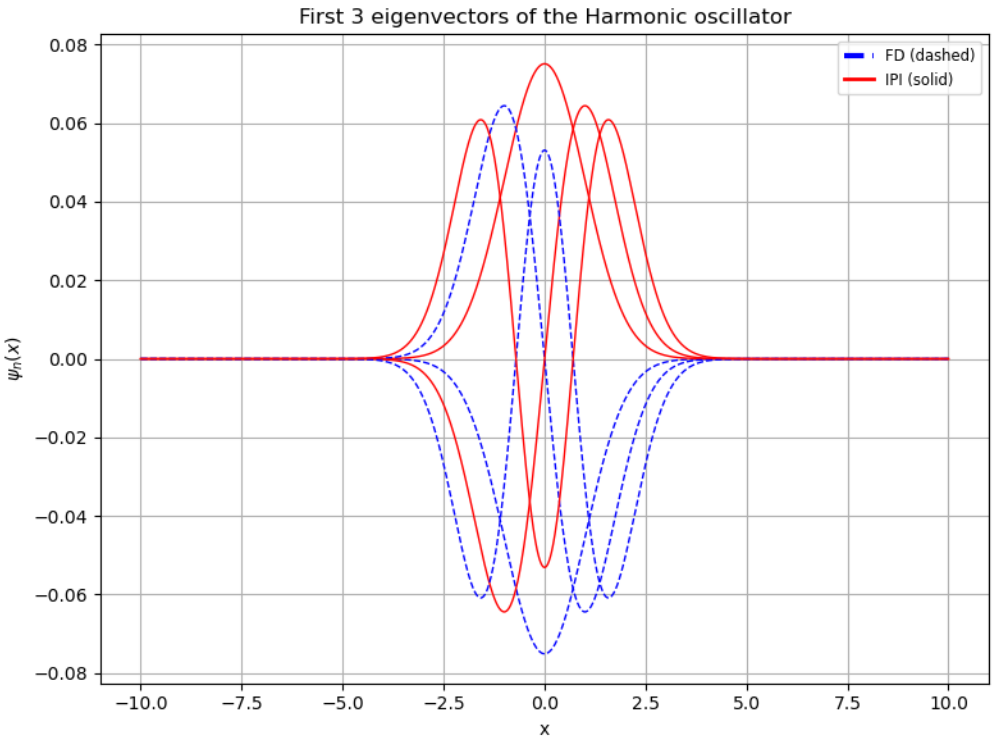

Figure 2: Comparison of the first 3 eigenvectors.

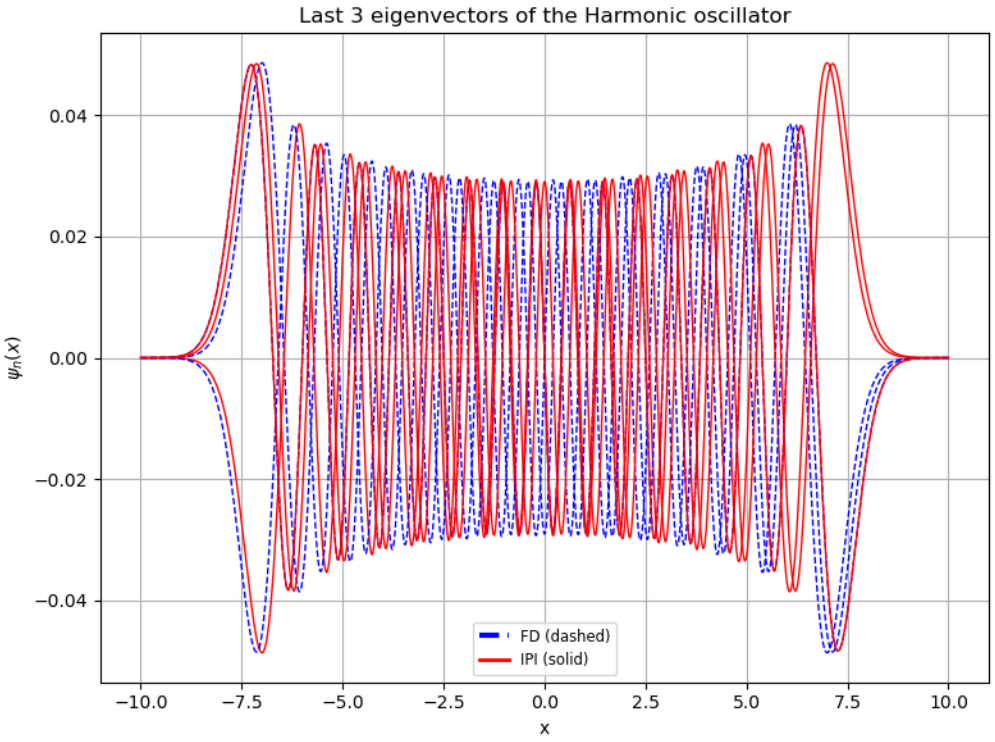

Figure 3: Comparison of the last 3 eigenvectors.

As shown in Figure 2, both methods accurately capture the expected symmetry and nodal structure of the harmonic oscillator eigenfunctions for the lowest states.
In Figure 3, we note that the overall agreement remains strong, but small deviations become more visible - especially near the boundaries - which is expected due to increased oscillatory behavior at higher excited states, hence greater sensitivity to discretization error and boundary effects.

4.3 Runtime

Since both methods produce accurate results, a good way to compare their efficiency is by comparing the computation time, the results are summarized below:

N_x	**FD** (ms)	**IPI** (ms)
40	7.2	5.9
100	8.4	6.9
500	57.1	7.1
1000	170.6	11.1
10 000	53.3 $\cdot 10^3$	76.8

Table 2: Computation time for the last five eigenvectors.

We note from Table 2 that at small grid sizes, the performance of both methods is comparable, with IPI being slightly faster. However, as the matrix size increases, the runtime for FD grows significantly, while the IPI method scales more efficiently.

4.4 Orthonormality of the eigenvectors

We also verified that the computed eigenfunctions from both methods satisfy the expected orthonormality conditions, that is, each eigenfunction fulfills:

$$\|\psi_n\|^2 = 1 \tag{36}$$

and the inner products between distinct eigenfunctions:

$$\langle \psi_n | \psi_m \rangle = \int \psi_n^*(x)\, \psi_m(x)\, dx \;\approx\; 0 \qquad \text{for} \qquad n \neq m \tag{37}$$

To verify the orthonormality numerically, we computed the overlap matrix $\Psi^\top \Psi$, which is given by:

$$\Psi^\top \Psi = \begin{bmatrix} \langle \psi_1, \psi_1 \rangle & \langle \psi_1, \psi_2 \rangle & \cdots \\ \langle \psi_2, \psi_1 \rangle & \langle \psi_2, \psi_2 \rangle & \cdots \\ \vdots & \vdots & \ddots \end{bmatrix} \tag{38}$$

If the eigenvectors $\{\vec{\psi}_i\}$ are orthonormal, then:

$$\langle \psi_i, \psi_j \rangle = \delta_{ij} \quad \Rightarrow \quad \Psi^\top \Psi = I \tag{39}$$

Which was the case for our methods, this matrices was numerically close to the identity, confirming that the eigenvectors form an orthonormal set.

4.5 Perturbed Harmonic oscillator

By establishing a reference point for comparison, we can now effectively evaluate the impact of the perturbations on the system's energy levels and wave functions.
Table 3 shows the energy of the first five states before and after perturbation.

n	$E_n/\hbar\omega$	$E_n^G/\hbar\omega$
0	1	3.18
1	3	3.49
2	5	6.87
3	7	7.60
4	9	10.41

Table 3: Energy values of the first 5 eigenstates before and after implementing the Symmetric Gaussian bump.

This perturbation leads to noticeable alterations in the energy eigenvalues. It is worth to note that since the perturbation potential is symmetric around the origin, the symmetric states (corresponding to even quantum numbers $n = 0, 2, 4, ...$) were the most affected. This observation is consistent with the properties of the wave functions.
To further shed light on the impact of perturbation on the quantum harmonic oscillator, figure 4 juxtaposes two sets of eigenfunctions side by side: the left figure shows the first five states of the unperturbed system, while the right figure shows the corresponding states after introducing the Gaussian perturbation.

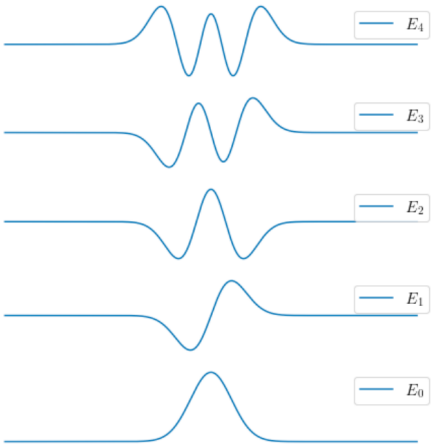

(a) Before implementing the bump.

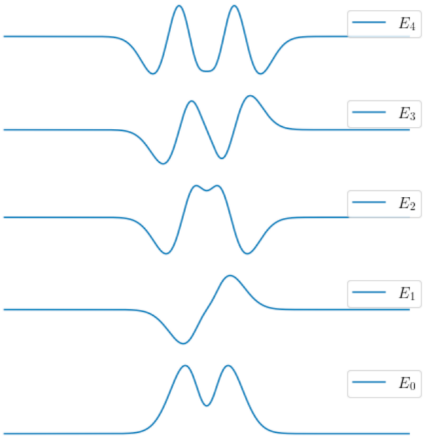

(b) After implementing the bump.

Figure 4: The first five eigenstates of the harmonic oscillator before and after implementing the Symmetric Gaussian bump.

5 Discussion and Conclusion

Both the finite-difference (FD) and inverse power iteration (IPI) methods produced accurate eigenvalues and eigenvectors for the quantum harmonic oscillator. The results closely matched analytical solutions with small deviations appearing only in higher-energy states. In conclusion, both FD and IPI were efficient for smaller matrices, but IPI became more efficient as the grid size increased.